STAR FORMATION IN THE BRIGHT RIMMED GLOBULE IC1396N

C. Codella[1], R. Bachiller[2], B. Nisini[3], and P. Saraceno[1]

[1]Istituto di Fisica dello Spazio Interplanetario, CNR, Area di Ricerca Tor Vergata, Via Fosso del Cavaliere 100, 00133 Roma, Italy
[2]Observatorio Astronómico Nacional (IGN), Apartado 1143, E-28800, Alcalá de Henares (Madrid), Spain
[3]Osservatorio Astronomico di Roma, Via di Frascati 33, 00040 Monteporzio, Italy

Abstract

The bright rimmed globule IC1396N has been investigated through a multiline survey at mm-wavelengths. In order to probe a wide range of physical conditions, emission due to CO, CS, DCO^+ and SiO has been observed. The present results, combined with previous ISO observations, allow to study how the presence of massive stars can affect the structure of the dense molecular clouds in the surroundings triggering the process of star formation. The occurrence of several bipolar molecular outflows and dense cores shows a quite complex scenario indicating that IC1396N hosts different regions where the star forming process is running. The results call for high angular and spectral resolution observations at submillimetre and infrared wavelengths tracing high excitation conditions throughout the globule making IC1396N an ideal target for the future FIRST mission.

Key words: ISM: clouds – ISM: jets and outflows – ISM: molecules – ISM: individual objects: IC1396N – Radio lines: ISM

1. Introduction

IC1396 is a well known extended H II region (S131, Sharpless 1959) located near the Cep OB2 association, at a distance of about 750 pc from the Sun. The region is ionized by the O6.5 star HD206267, the brightest member of the young cluster Trumpler 37. Several globules have been identified in IC1396 through Hα images (Osterbrock 1957). In particular, IC1396N is a cometary globule with a bright rim located at $\sim$ 11 pc from HD206267 and is through to be site of star formation. Actually, it hosts IRAS21391+5802, strong H_2O maser sources (Tofani et al. 1995, Slysh et al. 1999) and an extended bipolar molecular outflow (Sugitani et al. 1989). The indication that stars can form in cometary globules has been already found for a limited number of targets (e.g. Sugitani et al. 1995, Lefloch et al. 1997, and references therein). However, the interest about IC1396N has recently increased due to observations at far-infrared (FIR) wavelengths with the Infrared Space Observatory (ISO). Such observations have unvealed a rich spectrum, with many lines of CO, OH and H_2O, indicating the presence within the globule of dense shocked regions excited at a temperature in excess of 1500 K (Saraceno et al. 1996). Thus, IC1396N has converted in one of the best laboratories where to investigate the mechanisms of star formation induced by the propagation of an ionization shock front, the so-called radiation driven implosion (RDI) mechanism (Reipurth 1983).

In this paper we present the preliminary results coming from a multiline survey (Codella et al. 2001) at millimeter wavelengths of the bright rimmed globule IC1396N, performed with the IRAM 30-m antenna. The main aims of this work are: (i) to carefully investigate the structure of the globule and of the bipolar outflow with high spatial and spectral resolution (through CO observations), (ii) to trace the high density structures (through CS and DCO^+) and the highest excitation conditions of the molecular outflow (through SiO), (iii) to study how the presence of massive stars can affect the structure of the dense molecular clouds in the surroundings triggering, at the same time, the process of star formation, (iv) to understand if the shocked gas observed with ISO is a consequence of the interaction of the mass loss process from Young Stellar Objects (YSOs) with the surrounding medium or is the result of the occurrence of the shock-wave associated with the H II region due to HD206267.

2. Observations

Observations with the IRAM 30-m telescope at Pico Veleta (near Granada, Spain) were carried out during several runs in November 1998 and January and May 1999. Table 1 summarizes the observed molecular species, the transitions, their rest frequencies and some observing parameters, such as the HPBW and the spectral resolution (dv). The main beam efficiency varies from 0.75 (at 90 GHz) to 0.37 (at 230 GHz). The observations were made by position switching. Pointing was checked every hour by observing nearby planets or continuum sources and it was found to be accurate to within $3''$. As spectrometers, an autocorrelator (AK) split into three parts was used to allow simultaneous observations of three different transitions. Moreover, also a 1 MHz filter bank, split into three parts of 2 $\times$ 256 and 512 channels, was used to allow simultaneous observations. The spectra were calibrated with the standard chopper wheel method and are reported here in units of main-beam brightness temperature ($T_{\rm MB}$).

Proc. Symposium *'The Promise of the Herschel Space Observatory'* 12–15 December 2000, Toledo, Spain
ESA SP-460, July 2001, eds. G.L. Pilbratt, J. Cernicharo, A.M. Heras, T. Prusti, & R. Harris

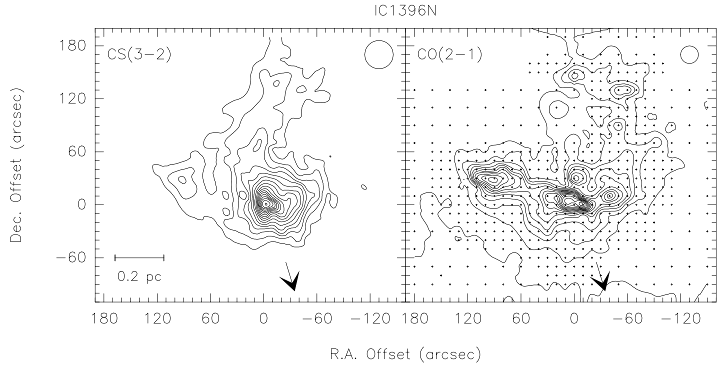

Figure 1. Contour maps of the integrated CO (J = 2–1) and CS (J = 3–2) emission towards IC1396N with superimposed the optical image reproduced from the POSS red plates. The empty circles show the IRAM beam (HPBW), the small crosses mark the observed positions, while the black arrows point out the direction where HD206267 is located. The CO contours range from 10.0 (∼ 10σ, where σ is the r.m.s. of the map) to 465.0 K km s^{-1} by step of 30.0 K km s^{-1}. The CS contours range from 2.5 (5σ) to 45.0 K km s^{-1} by step of 2.5 K km s^{-1}.

Table 1. List of molecular species, transitions and observing parameters.

Transition	ν_o (MHz)	HPBW ($''$)	dv(AK) (km s^{-1})	dv(1MHz) (km s^{-1})
SiO(2–1)	86847.0	29	0.13	3.45
CO(1–0)	115271.2	21	0.10	2.60
SiO(3–2)	130268.7	18	0.17	2.30
DCO$^+$(2–1)	144077.3	16	0.21	—
CS(3–2)	146969.0	16	0.32	2.04
SiO(5–4)	217104.9	11	0.11	1.38
CO(2–1)	230538.0	10	0.10	1.30

3. Results and discussion

3.1. The globule and the outflows

Figure 1 shows the maps of the integrated CO J = 2–1 and CS J = 3–2 emissions, centred at α_{1950} = 21$^{\rm h}$ 39$^{\rm m}$ 10$\overset{\rm s}{.}$3, δ_{1950} = +58° 02′ 29″, i.e. the coordinates of IRAS21391+5802. The maps reveal the cometary nature of the globule, with a remarkable head-tail structure and a total length of 0.8 pc. Figure 2 reports the channel map of the CO J = 2–1 emission, allowing to study the gas kinematics. The ambient LSR velocity emission is centred around the −1.5 and +1.5 km s^{-1} panels (underlined by thicker boxes). It is possible to see that: (i) high velocity blue- and redshifted emission is coming from a bipolar jet-like structure symmetrically located with respect to the IRAS21391+5802 coordinates, (ii) there is a significant spatial overlap between the blue and the red emissions, (iii) other two high velocity elongated components located along a direction similar to that of the structure individuated around the IRAS counterpart are detected at about Dec. Offset = +140″. We conclude that IC1396N is associated with at least two molecular outflows: that located around the (0″,0″) position, hereafter called central outflow, and that located around the (–30″,+140″) offset, hereafter called northern outflow. The length of the central and the northern CO outflows is about 0.7 and 0.3 pc, while the collimation factor (ratio between length and width) is ∼ 4.5 and 3, respectively. Four clumps associated with the central outflow (pointed out in the channel maps) have been detected: SE1 (+90″,+30″), SE2 (+10″,0″), SW2 (0″,0″) and SW1 (–40″,+10″). On the other hand, the northern outflow shows a blueshifted lobe, NW, at (–60″,+130″) and a redshifted component, NE, at (0″,+150″).

Although the central outflow was previously known, the present data provide the first clear evidence for the existence of a bipolar molecular outflow in the northern region of IC1396N. The central bipolar outflow in IC1396N was previously studied by Sugitani et al. (1989). However, the data reported here provide new interesting information on its structure. The clumpy structure suggests that episodic events of the mass loss process have occurred. The outflow morphology suggests that the driving source has to be located very close to the (0″,0″) offset, i.e. around the IRAS coordinates.

The central outflow has a total mass of 0.1 $M_\odot$ equally distributed between the red and the blue lobes. In order to value the kinematical outflow parameters, the inclination (θ) to the plane of the sky has to be assumed. Unfortunately, the present observations do not allow a good θ estimation. However, taking a compromise between the quite elongated structure of the outflow and the overlap between the two lobes, it is reasonable to assume a low θ value, probably in the 10°-20° range. For orientation, we give the kinematical parameters for θ = 20°. Thus, the estimate of the momentum and the kinetic energy gives P = 1.9 $M_\odot$ km s^{-1} and $E_{\rm kin}$ = 5 10^{44} erg, respectively. A

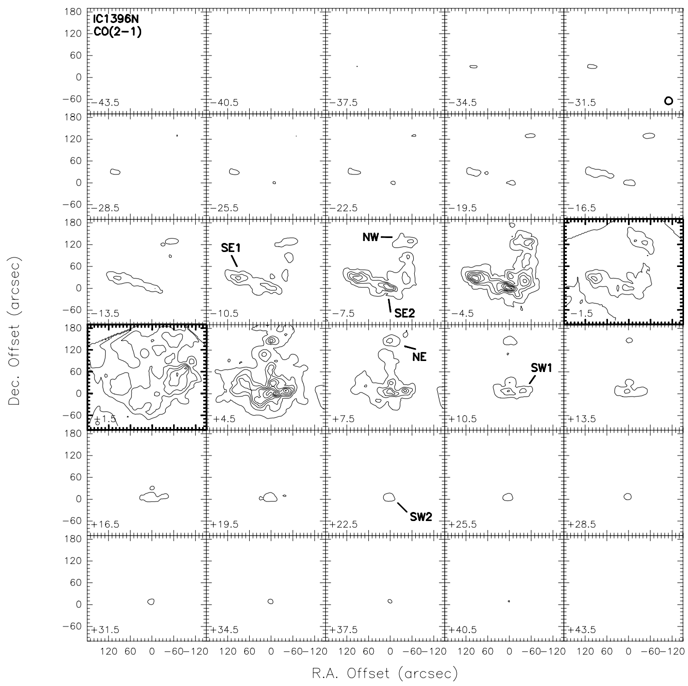

Figure 2. Channel map of the CO J = 2–1 emission towards IC1396N. Each panel shows the emission integrated over a velocity interval of 3 km s^{-1} centred at the value given in the left corner. The thick boxes point out the ambient velocity emission. Symbols are drawn as in Fig. 1, while the labels underline different components of the molecular outflow. The contours range from 3.00 ($\sim 5\sigma$) to 87.00 K km s^{-1} by step of 12.00 K km s^{-1}.

kinematical timescale of $\simeq 3\ 10^4$ yr has been valued, allowing to deduce the force required to drive the mass loss process, $F = 6.9\ 10^{-5}\ M_\odot$ km s^{-1} yr^{-1}, the mass loss rate, $\dot{M} = 3.2\ 10^{-6}\ M_\odot$ yr^{-1}, and the mechanical power, $L_{\rm m} = 0.15\ L_\odot$. Note, however, that $L_{\rm m}$ increases to 1.20 $L_\odot$ if the inclination angles changes to 10°.

With a mass of only $\sim 0.01\ M_\odot$, the northern outflow is found to be an order of magnitude less massive than the central one. Taking into account the definite spatial separation between blue and red emissions, we estimate that the inclination angle of the outflow to the plane of the sky is about 10°. The outflow momentum is $P = 0.4$ $M_\odot$ km s^{-1} and its kinetic energy 2.4 10^{44} erg. Moreover, the estimate of the kinematical timescale ($\sim 1.7\ 10^4$ yr) suggests that the northern outflow is significantly younger than the central one. The force is of the northern outflow is 3 $10^{-5}\ M_\odot$ km s^{-1} yr^{-1}, its mass loss $\simeq 6\ 10^{-7}\ M_\odot$ yr^{-1} and its mechanical power 0.19 $L_\odot$.

3.2. SiO emission from the central outflow

In order to clarify the structure of the high velocity gas components of the IC1396N central outflow, a standard tracer such as SiO has been used. Figure 3 shows the velocity channel maps of the J = 5–4 emission, e.g. that observed with the best spectral and spatial resolution. Silicon monoxide is present only along the main axis. It is possible to clearly observe the elongated structure of the outflow, with the four clumps detected in CO. The collimation factor is about 6, i.e. a value somewhat larger than that derived using CO, confirming that SiO, with respect carbon monoxide, can trace the inner part of the outflow.

An estimate of the central outflow age can be derived using the position of the SiO SE1 and SW1 clumps, assuming its inclination on the plane of the sky and that the material traveled from the driving source to the present location with a velocity of $\sim$ 8 (SW1) and 11 km s^{-1} (SE1). We find $\tau \simeq 7\ 10^3$ (SW1) and 2 10^4 yr (SE1), i.e. values which are reasonably in agreement with the outflow age derived from CO.

3.3. High density cores

The CS observations allow to detect the high density molecular clumps hosting the driving sources of the two molecular outflows. In the central region of IC1396N the clump size is about 0.18 pc (Fig. 4), while where the northern outflow is present, the clump is located inside a quite elongated structure $\simeq$ 0.16 pc wide. The CS column density is $\sim 2\ 10^{14}$ and 10^{13} cm^{-2} for the central and the northern clump, respectively. The distribution of the ambient material of the central region has been investigated also using DCO^+ emission: at least three unresolved ($\leq$ 0.07 pc) clumps have been detected at different velocities in the same region traced by CS. The typical DCO^+ column density is about 3 10^{12} cm^{-2}.

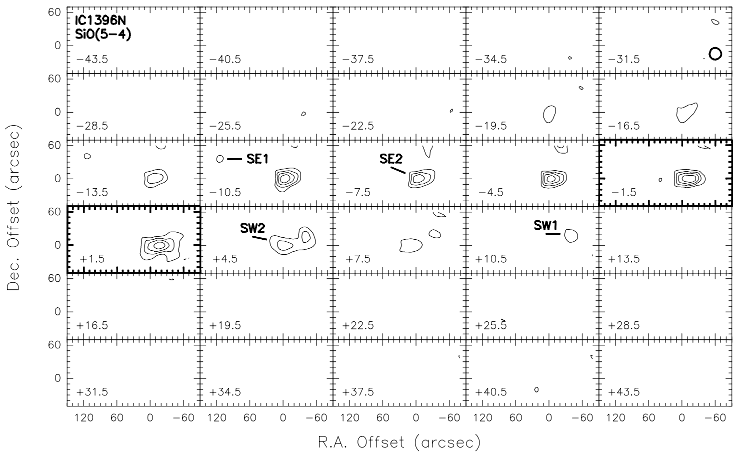

Figure 3. Channel map of the SiO J = 5–4 emission towards IC1396N. Each panel shows the emission integrated over a velocity interval of 3 km s^{-1} centred at the value given in the left corner. Symbols are drawn as in Fig. 1. The contours range from 0.3 (∼ 3σ), to 1.2 K km s^{-1} by step of 0.3 K km s^{-1}.

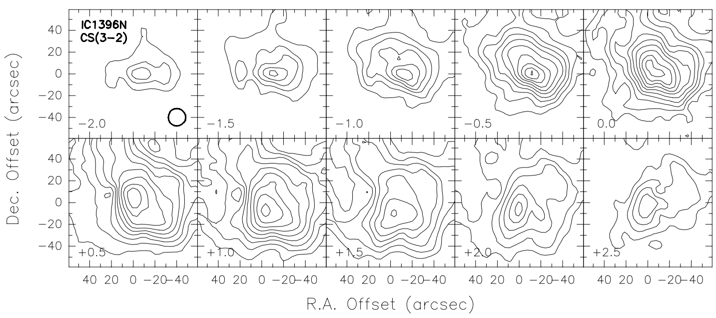

Figure 4. Channel map of the CS J = 3–2 emission towards the IC1396N central region. Each panel shows the emission integrated over a velocity interval of 0.5 km s^{-1} centred at the value given in the left corner. Symbols are drawn as in Fig. 1. The contours range from 0.4 (∼ 5σ), to 4.0 K km s^{-1} by step of 0.4 K km s^{-1}.

4. FIRST perspectives

In the region of the globule between the central and the northern outflows, roughly around the (–30″,+90″) position, red- and blueshifted extended structures are clearly detected at velocities relatively close (≤ ±10 km s^{-1}) to the ambient one. In addition, a red clump at (0″,+30″) and a blue one at (–40″,+20″) are observed. This emission could indicate the occurrence of other outflows, as supported also by the detection at near IR wavelengths of faint H_2 knots (Nisini et al. 2001). These results, together with the ISO detection of shocked material, indicate that the process of star formation occurs throughout the globule and make IC1396N an ideal target for the future FIRST observations. With the three instruments, FIRST will allow to trace, with a definitely higher spatial and spectral resolution with respect to ISO, the gas excitation ranging from few tens of kelvins to more than 2000 K, and to study the energetic of the infall-outflow phenomena associated with the young stellar objects.

References

Codella C., Bachiller R., Nisini B., Saraceno P., Testi L., 2001, A&A, submitted

Lefloch B., Lazareff B., Castets A., 1997, A&A 324, 249

Nisini B., Massi F., Vitali F., et al., 2001, in preparation

Osterbrock D.E., 1957, ApJ, 125, 622

Reipurth B., 1983, A&A, 117, 183

Saraceno P., Ceccarelli C., Clegg P., et al., 1996, A&A, 315, L293

Sharpless S., 1959, ApJS, 4, 257

Slysh V.I., Val'tts I.E., Migenes V., et al., 1999, ApJ, 526, 236

Sugitani K., Tamura M., Ogura K., 1995, ApJ, 455, L39

Sugitani K., Fukui Y., Mizuno A., Ohashi N., 1989, ApJ 342, L87

Tofani G., Felli M., Taylor G.B., Hunter T.R., 1995, A&AS, 112, 299